Water network dynamics at the critical moment of a peptide's β-turn formation: A molecular dynamics study

George Karvounis, Dmitry Nerukh, and Robert C. Glen

View Online   Export Citation

ARTICLES YOU MAY BE INTERESTED IN

Molecular dynamics with coupling to an external bath
The Journal of Chemical Physics **81**, 3684 (1984); https://doi.org/10.1063/1.448118

A smooth particle mesh Ewald method
The Journal of Chemical Physics **103**, 8577 (1995); https://doi.org/10.1063/1.470117

The Journal of Chemical Physics 2018 EDITORS' CHOICE READ NOW!

AIP Publishing

Water network dynamics at the critical moment of a peptide's β-turn formation: A molecular dynamics study

George Karvounis, Dmitry Nerukh, and Robert C. Glen
Unilever Centre for Molecular Informatics, Department of Chemistry, Cambridge University, Cambridge CB2 1EW, United Kingdom

All-atom molecular dynamics simulations for a single molecule of Leu-Enkephalin in aqueous solution have been used to study the role of the water network during the formation of β-turns. We give a detailed account of the intramolecular hydrogen bonding, the water-peptide hydrogen bonding, and the orientation and residence times of water molecules focusing on the short critical periods of transition to the stable β-turns. These studies suggest that, when intramolecular hydrogen bonding between the first and fourth residue of the β-turn is not present, the disruption of the water network and the establishment of water bridges constitute decisive factors in the formation and stability of the β-turn. Finally, we provide possible explanations and mechanisms for the formations of different kinds of β-turns. © *2004 American Institute of Physics.* [DOI: 10.1063/1.1780152]

I. INTRODUCTION

Proteins are strongly influenced by the behavior of the surrounding solvent. Water has a significant impact on the structure, stability, and dynamics of a protein as determined from experiment and computer simulations. It has been shown that there is a minimum amount of water necessary for the biological function of a protein.[1] It has also been established that the properties of water molecules in the vicinity of a protein's biological waters[2] differ significantly from those of the bulk water. Detailed information on water structure and dynamics, which is available from molecular dynamics (MD) simulations, can shed light on the role of water in protein structure and function at an atomic level.

Numerous theoretical studies have analyzed the hydration and the structural properties of proteins and peptides but in most cases, either static models or unfolding procedures (for larger proteins) were used and averages over long periods were taken. However, folding emergences in a transition-like fashion with critical moments of only 1–2 ps long. The mechanisms of these transitions are not well understood and, to the best of our knowledge, not many studies are devoted to this key process. Therefore, we believe that the detailed analysis of the water-peptide system during these critical periods will significantly advance the knowledge of peptide and protein folding mechanisms.

Beck *et al.* investigated the solvation properties for all 20 L-amino acids using different tripeptide motifs simulated for 0.3 μs,[3] whereas others[4] have unified experimental and theoretical methods to characterize the interactions between aminoacids and aqueous solvent. Other groups have used MD simulations to study the water molecules that penetrate and escape from protein hydration sites[5,6] or the water dynamics near the protein surface.[7,8] All these studies have emphasized the role of the water network surrounding protein hydration sites of particular amino acid residues.

Enkephalins are pentapeptides that act as neurotransmitters in the central nervous system, being endogenous opioid peptides with morphine-like activity. Many research groups have used them as models for studies aimed at developing highly selective antagonists for use as pharmacological tools in opioid research.[9] Previous MD and NMR studies of the enkephalins demonstrate that this highly flexible solvated peptide runs through a large range of conformations on the nanosecond time scale.[10]

The study of small peptides such as Leu-Enkephalin (Fig. 1) and Met-Enkephalin is important from several perspectives.[11] They encapsulate protein-like features better than smaller molecules (e.g., *N*-methyl acetamide) and are computationally accessible (long MD simulations in water over a relevant time scale) in contrast to even small proteins. MD simulation of small peptides in water may offer insight into the folding problem if it is long enough to demonstrate reproducibly the experimentally observed phenomena (e.g., turn formation).

An excellent review of both experimental and theoretical studies of the structural aspects of the Leu-Enkephalin using a range of initial configurations and different solvation models was published by the GROMOS group.[12] This review gives a comprehensive account of the backbone and side chain conformations indicating the existence of β-turns and bends formed during the simulation. Aburi and Smith[13] have also applied MD methods to investigate the conformation of Leu-Enkephalin as a function of pH. Abdali *et al.*[14] used Density Functional Theory (DFT) calculations to verify a single-bend conformation. Both these groups utilized all-atom MD simulations in which the peptide started from its extended configuration.

The main area of research in our group involves the investigation of the dynamic complexity of molecular processes.[15] The approach focuses on the phase-space trajectory of a molecular system to elucidate the rules and regularities of the underlying dynamics that lead to self-organising, emergent behavior. We are particularly interested in applying similar complexity analysis methods to gain a better understanding of the mechanisms of protein folding. It
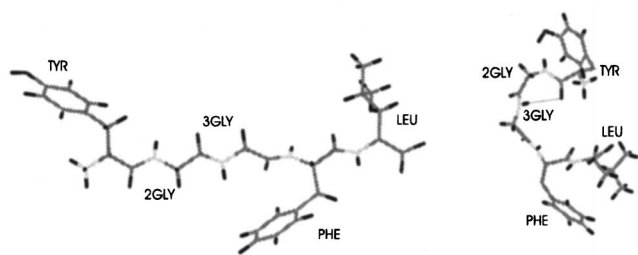
FIG. 1. The extended and folded conformation of Leu-Enkephalin. Notice the hydrogen bond between TYR and 3GLY.

is not feasible to deal with the complexity of the whole $6N$-dimensional phase-space trajectory and a proper, representative subspace should be considered. Here, we have examined the water dynamics of a β-turn formation with a view to identifying suitable data that can be used in the calculation of the complexity of the system.

Despite continuous experimental advances, the process of solvation in aqueous media remains a highly complex phenomenon to describe and explain. Various interactions between solvent and solute along with rearrangements of the solvent density and network through the disruption/forming of hydrogen bonds in the vicinity of the solute are examples of factors that underlie these complications. The contribution of the water network rearrangement towards the peptide's structure was also identified by Smith and Pettitt[16] who have studied the solvent structure of the bis(penicillamine) enkephalin zwitterion, a system similar to the Leu-Enkephalin peptide.

Most of the above studies investigate the role of water over an extended time interval, using radial distribution functions, mean residence times, and other averaged parameters. Our approach however, analyzes the water dynamics at the specific moment of the β-turn formation. We want to infer the causality of both peptide and water dynamical changes at the moment of the β-turn structure emergence. Therefore, although we performed five 3 ns long simulations in order to identify the stable β-turns, our results and discussions are focused at the specific structural transition periods, as defined by geometric criteria. The time period used is ~4 ps which, as shown later, covers the period of three regimes: before the β-turn, quick transition, and stable turn.

To summarize, all-atom MD simulations started from the extended configuration. Four out of five simulations (labeled I, II, III, and IV) reveal the existence of two stable β-turns; the 1TYR-4PHE (1–4 β-turn) and the 2GLY-5LEU (2–5 β-turn). The existence of these turns is in general agreement with the studies of the previously mentioned research groups.[12] We present an analysis of the impact of water dynamics on the β-turn formations and report the orientation patterns and mobility parameters of the water molecules. In most simulations, the role of water bridging was decisive for the compact structure of the peptide. We will describe these cases in turn and finally we will deduce a general mechanism for all the observed simulations.

II. METHODS

For each simulation, the Leu-Enkephalin molecule (NH_3^+-TYR-GLY-GLY-PHE-LEU-COO$^-$) was built using SYBYL 6.9 (Ref. 17) in a linear conformation and in a zwitterionic form (with N-terminal NH_3^+ and C-terminal COO$^-$). It was solvated in a rectangular box of 5826 SPC (Ref. 18) water molecules. The aim was to obtain a continuous trajectory of the coordinates, avoiding the ''jumps'' caused by periodic boundary conditions (which would create difficulties for the later calculation of complexity). After solvation, the system was energy minimized using the steepest descent method for 500 steps. The GROMOS96 (Ref. 19) force field was used. All five simulations were 3 ns long (of 0.002 ps time steps), performed with weak coupling to a water bath of constant temperature at 300 K (peptide and solvent individually), with a coupling time of 0.1 ps. Pressure coupling was also applied to a pressure bath with reference pressure of 1 bar and a coupling time of 0.1 ps.[20] All bond lengths of the peptide were constrained using the SHAKE (Ref. 21) algorithm. The SETTLE (Ref. 22) algorithm was used to constrain the bond lengths and angles of the SPC waters. The simulations were performed using GROMACS.[18] A 1 nm cutoff distance for both van der Waals and Coulomb potentials was used. The system was allowed to equilibrate for the first 100 ps followed by snapshots of the dynamics at every 20 ps for the rest of the simulation. At the critical point of turn formation we examined the system step by step for a period of 4 ps (2000 steps).

III. RESULTS

A. Overall peptide's dynamics

To characterize the overall secondary structure of the peptide, we have adopted the general definitions of the PROMOTIF program.[23] A β-turn is defined for four consecutive residues if the distance between the C_α atom of residue i and the C_α atom of residue $i+3$ is less than 7 Å and if the two central residues are not helical (Fig. 2). We want to emphasize that for three of these simulations (simulations II, III, and IV) the β-turn remains stable for more than 400 ps. At simulation I, the 1–4 β-turn remains stable for ~300 ps, to be followed by a stable 2–5 β-turn.

The above turns are the result of a quick structural transition. In fact, as it is already mentioned, in all cases we used the extended chain as a starting configuration. A hydrophobic collapse took place shortly after, enhanced by the aromatic nature of the Tyrosine and Phenylalanine residues. This collapse created the conformational scaffold for a more compact structure. At a critical point, the system suddenly folds even further, to form the β-turns. There are no obvious reasons, from the peptide's point of view, for the character of this transition. However, we observe a specific folding regime (β- turn) emerging from an essentially chaotic system. Therefore, it is more appropriate to concentrate our analysis at specific moments of conformational transition, than to perform extensive conformational or cluster analysis throughout the entire β-turn.
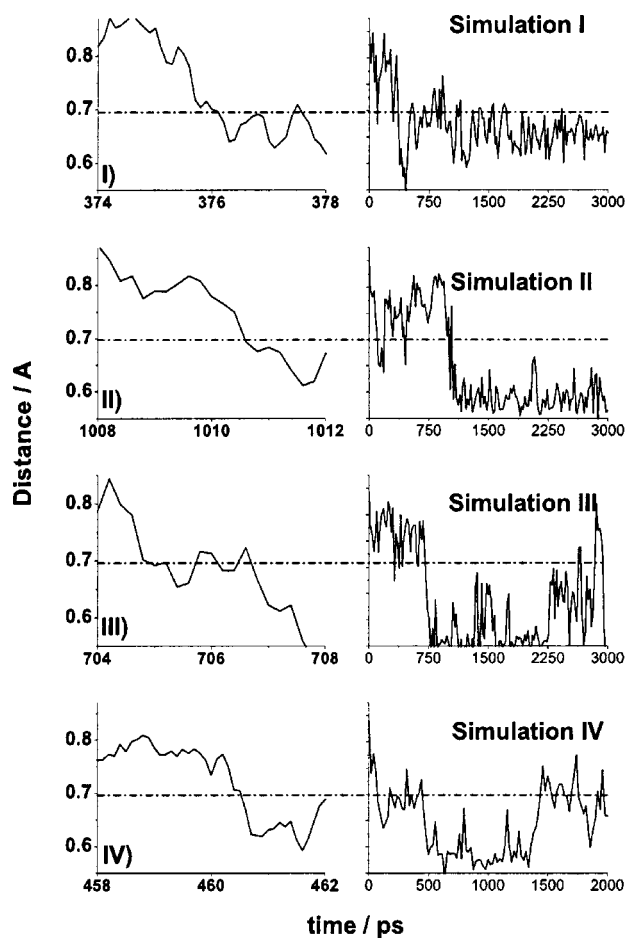
FIG. 2. The i to $i+3$ C_α distances taken from four different simulations. The dotted line denotes the β-turn threshold: the distance is at 7 Å. Notice how the transitions of simulations I and IV are sharper than the other simulations. This is attributed to strong water bridging and intramolecular hydrogen bonding. The stability of the turns can be seen at the graphs on the left. For most of the simulations, the β-turn remains stable for more than 400 ps. For the first simulation, we concentrate at the first transition point (~376 ps). For simulation IV we show the first 2000 ps.

B. Intramolecular H-bonding during the β-turn formation

Before analyzing the results of the simulations, it is necessary to define the terms used to describe the computed structural features. Despite the common use of the term "hydrogen bonding," its definition remains somewhat ambiguous. The problem is not only technical, but also a conceptual one. The criteria can include: geometrical parameters,[24,25] energies,[26] and kinetics.[27] For the elucidation of the intramolecular hydrogen bonding we have implemented the DSSP electrostatic model.[26] In this algorithm, hydrogen bonding is established when donors and acceptors are within a defined *hydrogen bond energy* threshold.

Figure 2 illustrates the β-turn formation in four different simulations. Notice the difference in the sharpness and the speed of the transition, particularly between simulation III, where we have found no strong intramolecular hydrogen bonds and water bridges, and simulations where many water bridges (simulation I) and intramolecular hydrogen bonds (simulation II) take place. It has been reported that 25% of all β-turns do not form a strong intramolecular hydrogen
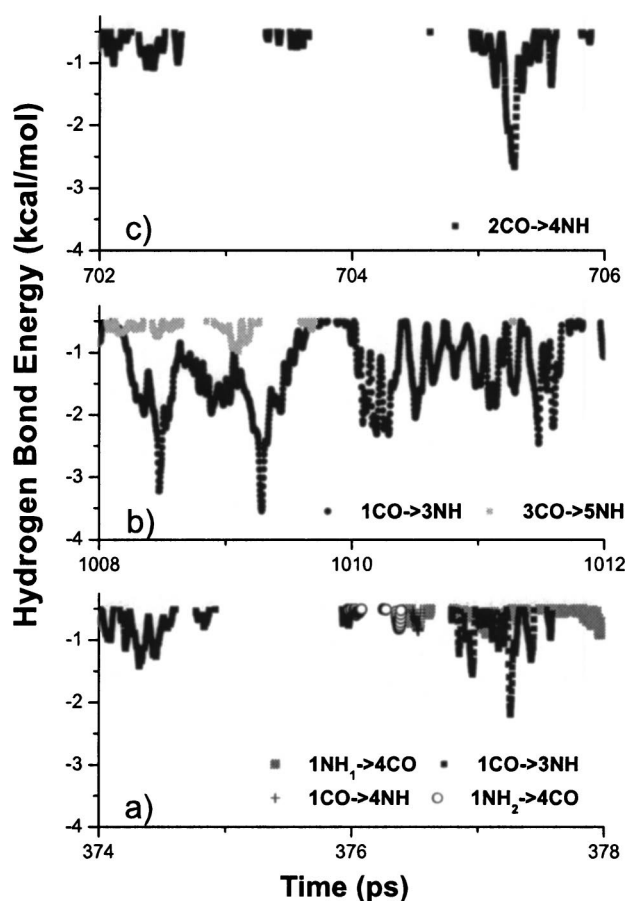

FIG. 3. Hydrogen bond energies calculated by the DSSP algorithm based on an electrostatic model. The three graphs correspond to three different simulations of an open β-turn. (a) and (b) correspond to a 1–4 β-turn and (c) to a 2–5 β-turn.

bond between the first and the fourth residue. These turns are often called "open" turns[28] and this is found to be the case in the first three β-turns (Fig. 2, I–III). Therefore, the "open" β-turns constitute the majority of the results of our simulations, and we will refer to those more extensively.

Theoretical and experimental studies[12] have reported that there is no significant hydrogen bonding between the i and $i+3$ residues of a β-turn. Figure 3 demonstrates the strength (in terms of energy) of the intramolecular hydrogen bonds. We notice that the energies of most of the hydrogen bonds have a small negative value (i.e., weak bonding), except for the $1CO \rightarrow 3NH$ interaction [Figs. 3(a) and 3(b)] and $2CO \rightarrow 4NH$ [Fig. 3(c)].

In all cases, although there is no sign of a strong $1 \rightarrow 4$ hydrogen bond (i.e., hydrogen bonding energy < -1 kcal/mol), there is a $1 \rightarrow 3$ hydrogen bond that stabilizes the backbone structure. All other hydrogen bonds shown in Figs. 3(a) and 3(b) are weak and insignificant.

In one simulation out of five, we had the effect of strong hydrogen bond formations between the i and $i+3$ residue during the moment of the turn. Figure 4 displays these bonds.

In this particular simulation we noticed the following case: initially, a strong salt bridge was formed between the terminal residues [Fig. 4(g)] and thereafter the peptide had a
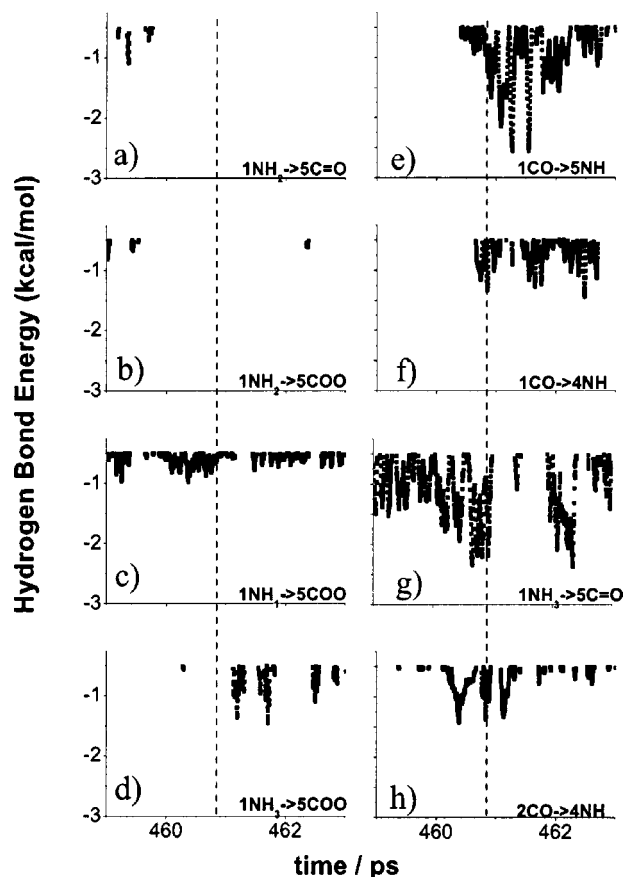
FIG. 4. Hydrogen bond energies calculated by the DSSP algorithm based on an electrostatic model for the simulation IV. Notice the strong intramolecular hydrogen bonds formed during the β-turn formation (d), (e), and (f). The dashed lines denote the moment of transition.

FIG. 5. (Color) Water-peptide hydrogen bonds. The blue layers correspond to the NH-OH$_2$ bonds and black to the CO-H$_2$O hydrogen bonds. At the top of the graphs three snapshots of before, during, and after the β-turn formation are shown. The differences in the water network and the different water bridges can be seen.

very compact configuration through the formation of strong intramolecular hydrogen bonds. Figures 4(d)–4(f) illustrate the hydrogen bonds between the carbonyl group of TYR and the amide groups of 4PHE and 5LEU.

Therefore, considering the lack of strong $1 \rightarrow 4$ hydrogen bonding for the majority of the simulations, we need to identify the factors that stabilize the β-turn. One of these factors appears to be the solvent-peptide interaction.

C. Water-peptide H-bonding during the β-turn formation

For all five simulations we have calculated the hydrogen bonding between the water molecules and the peptide using geometrical criteria (see Appendix A). They all produce similar patterns. To elucidate some common principles, we will concentrate on the water-peptide hydrogen bond pattern of simulation I and draw from this some general conclusions.

There is a dense water-peptide hydrogen bond network around the terminal residues (Fig. 5, TYR and LEU). This is due to the strong electrostatic interactions between the negatively charged 5LEU-COO$^-$ atoms and water hydrogens and between the positively charged 1TYR-NH$_3^+$ atoms and water oxygens. After the β-turn formation in simulation I ($\sim$376 ps), instead of numerous, short-lived hydrogen bonds, we notice fewer but stronger interactions. This is an indication
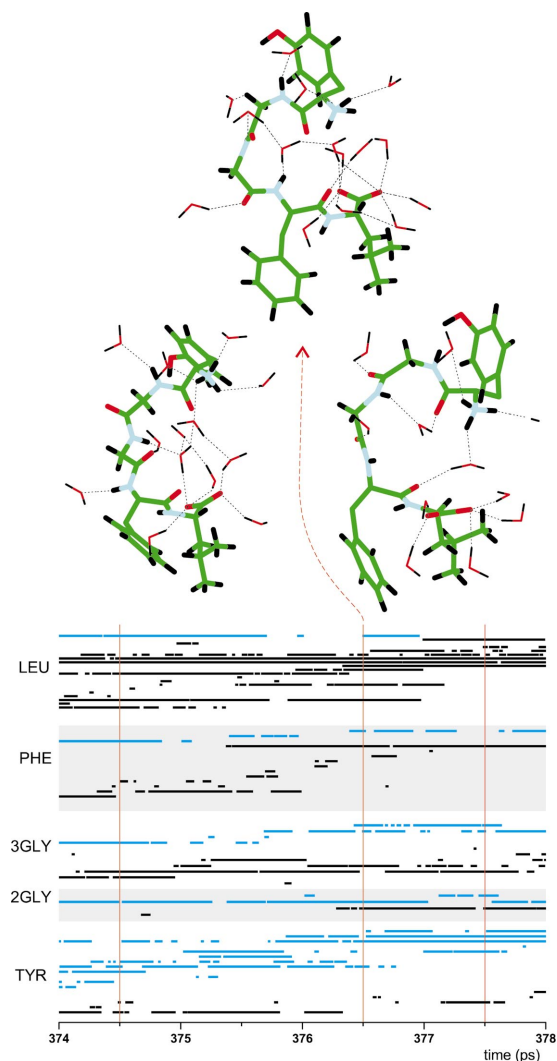
of the water network rearrangement until the turn is actually established. This observation applies also for PHE.

Figure 5 illustrates that 2GLY-NH is continuously hydrogen bonded to a water molecule. On the other hand, 2GLY-CO creates a stable hydrogen bond at the time of β-turn formation. 3GLY and especially 3GLY-CO are also involved with a long-lived water-residue hydrogen bonding event.

To investigate further the peptide-water interactions, Fig. 6 demonstrates three different kinds of bridging between the water molecules and the residues. In Fig. 6, (a) corresponds to water molecules bridging the same residue, (b) corresponds to water bridges shared by two *adjacent* residues, and finally (c) illustrates all the water bridges between distant residues. We present the water bridge pattern of two "open" β-turns, a 1–4 (graphs a1, b1, c1) and a 2–5 β-turn (graphs a2, b2, c2). The ellipses indicate the important water bridges that stabilize the two turns.

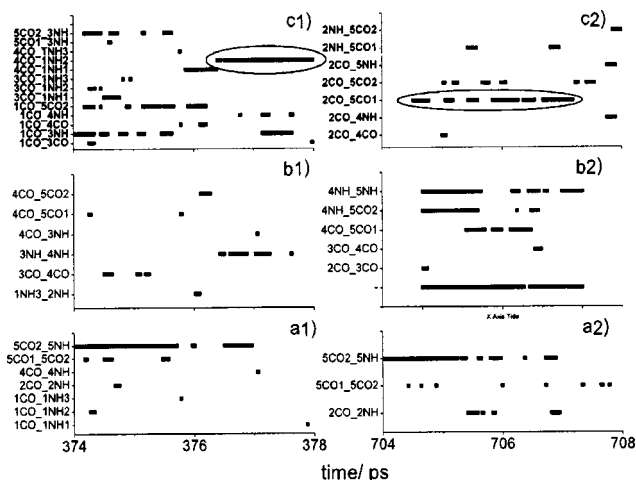In Fig. 6, graph a1, the most distinctive feature is the

FIG. 6. Water bridging between (a) the same residue, (b) between neighboring residues, and (c) between distant residues. Notice in graph c1 the 1–4 water bridge and in c2 the 2–5 bridge.

FIG. 7. Leu-Enkephalin's $\langle \alpha \rangle$ and the standard deviation of α at (a) 3.5 Å, (b) 3–4.5 Å. The upper curve corresponds to $\langle \alpha \rangle$ and the one below to the standard deviation.

water bridge shared within LEU. At the critical point of the β-turn formation though, this bridge breaks, adjusting to the water network reorientation and allowing more backbone flexibility. The same feature is observed in Fig. 6, graph a2, this time for the 2–5 β-turn. In Fig. 6, graph b2, we notice the water bridges between 4PHE and 5LEU that are seen to be breaking at the transition instant.

From Fig. 6, graph c1, before the critical moment of 376.2 ps, two important water bridges are formed. The first between 1CO and $5COO^-$ that disappears after the β-turn is formed and the other between 1CO and 3NH. Around 376.2 ps, the water bridge between 4CO and 1NH appears, starting with the first amine hydrogen and then moving to the second one (ellipse). It is worth mentioning that the latter water bridge stays intact for more than 1.5 ps. In Fig. 6, graph c2, the ellipse emphasizes the formation of water bridges between 2GLY and 5LEU that lead to the formation of the 2–5 turn.

D. Orientation of water molecules during the β-turn formation

We calculated an angle $\langle \alpha \rangle$ which represents the water orientation averaged over all water molecules within a particular shell (for more details see Appendix B). When $\langle \alpha \rangle < 90°$, a water oxygen's lone pairs are directed towards the reference point and when $\langle \alpha \rangle > 90°$ the lone pair points away from it.

To distinguish between the dynamics of "random" and "structured" water, the standard deviation of α in each shell was calculated (see Appendix B). If the standard deviation is $< 39.8°$, we will assign water as "structured" since it exhibits a monomodal distribution, if it is $> 39.8°$ water has a multimodal distribution.[31]

Assigning the 3GLY's backbone hydrogen (N-H) as our reference point, we calculated $\langle \alpha \rangle$ and standard deviation for the whole peptide. Although the results are similar for the majority of the simulations, we are going to illustrate the findings of simulation I that led to a 1–4 β-turn. In Fig. 7,
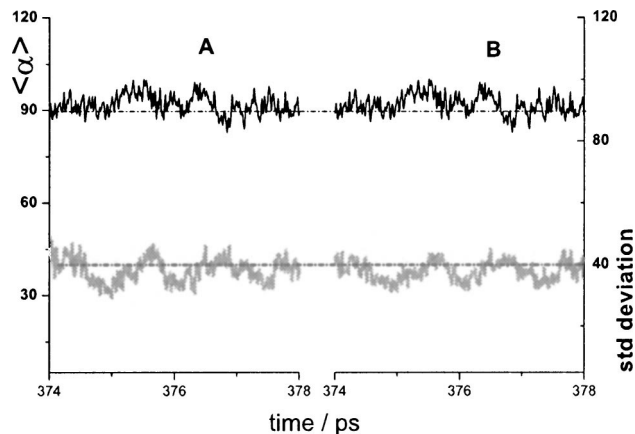
the upper curve corresponds to $\langle \alpha \rangle$ and the one below to the standard deviation.

Figure 7 highlights that when an average is taken over the whole peptide, important information about the specific regional orientation of water is lost. Therefore, to draw a more useful result, we have considered each residue in turn.

Figure 8 illustrates a particular trend (black line), an ascending behavior, starting from the positively charged TYR and ending at the negatively charged LEU. This was expected as the water oxygens orient their lone pairs away from the residue as they approach the negatively charged environment. Furthermore, it is also expected for the terminal charged residues to have more "structured" surrounding water molecules due to strong electrostatic interactions. For 5LEU the $\langle \alpha \rangle$ values remain well above 90° for all distances, especially at the second shell (Fig. 8, graph e2). Also, the standard deviation remains below 39.8°, which indicates that the water molecules are organized pointing their lone pairs away from the residue. There is no clear sign that the orientation of water molecules changes during the β-turn formation.
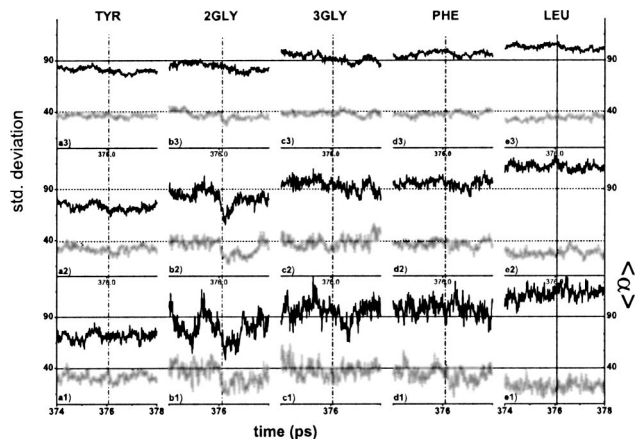

FIG. 8. $\langle \alpha \rangle$ and standard deviation of each residue (from bottom to top) up to 3.5 Å, 3–4.5 Å, 5–7 Å. The reference points are the hydrogens of the NH group of each residue. The (top) black curves correspond to $\langle \alpha \rangle$ and the (bottom) gray ones to the standard deviation. The vertical lines designate the β-turn formation moment.

For the positively charged NH_3^+ group, the $\langle\alpha\rangle$ and standard deviation values are similar for all three hydrogen atoms. Therefore, we will only present the data for one of the hydrogens. It is clear (Fig. 8, graph a1) that the $\langle\alpha\rangle$ values lie below 90; i.e., the water oxygen lone pairs point towards the residue on average (Fig. 8, graphs a1, a2, a3). The first shell water molecules undergo different stages of organization, sometimes less, sometimes more "structured" behavior. This behavior can be partially attributed to the presence of the polar side chain. Again, there is no sign of a specific influence of the β-turn formation around 376 ps.

The water molecules around 4PHE (Fig. 8, graphs d1, d2, d3) orient their oxygen lone pairs, on average, away from the residue at all distances (it is hydrophobic). After the moment of the β-turn formation (376–376.5 ps), the waters reach the minimum standard deviation, while $\langle\alpha\rangle$ is $\sim$100° (Fig. 8, graph d1). This signifies that at this particular time, most water molecules point away from the residue. At the second shell (Fig. 8, graph d2) this effect is smoother but still exists.

The water molecules surrounding 3GLY (Fig. 8, graphs c1, c2, c3) are randomly oriented, pointing their oxygen lone pairs both away and towards the residue. On average they have a slight tendency to point away, as $\langle\alpha\rangle>90°$ (Fig. 8, graphs c1, c2).

For residue 2GLY (Fig. 8, graphs b1, b2, b3), we observe a rapid change of $\langle\alpha\rangle$ and most importantly, of the standard deviation. Considering the first shell (Fig. 8, graph b1), the water molecules switch from an almost random orientation to a significantly more structured organization with the oxygen lone pairs pointing towards the residue. The standard deviation reaches a minimum, which implies that this is a cooperative motion of the water molecules. Interestingly, this feature is more profound at the second shell (Fig. 8, graph b2), where a drop of $\langle\alpha\rangle$ together with low standard deviation values suggests a rapid change of the water orientation. This drop is also visible, to a lesser extent, at a greater distance (Fig. 8, graph b3).

This rearrangement of the water orientation surrounding the glycine residues (2GLY or 3GLY) was observed in other simulations in both the first and second solvation shells (Fig. 9).

Figure 9 illustrates the $\langle\alpha\rangle$ of three simulations leading to a fast "open" β-turn (Fig. 9, simulation I), a slow open β-turn (Fig. 9, simulation II), and a fast turn with strong intramolecular hydrogen bonds (Fig. 9, simulation IV). Notice that in the cases of a fast transition, the reorientation at the moment of the β-turn formation is more profound.

To validate this observation, we examined whether this behavior was an artifact. Since an average is taken over water molecules, a sufficient number is required to make reasonable conclusions. It was found that the number of water molecules around 2GLY or 3GLY are from 5 to 8 for the first shell and from 9 to 14 for the second shell. In both cases there are enough water molecules for the calculation of averaged orientations. Furthermore, if an artifact was to be present at 2GLY then the same artifact would be present around 3GLY, which is not the case.

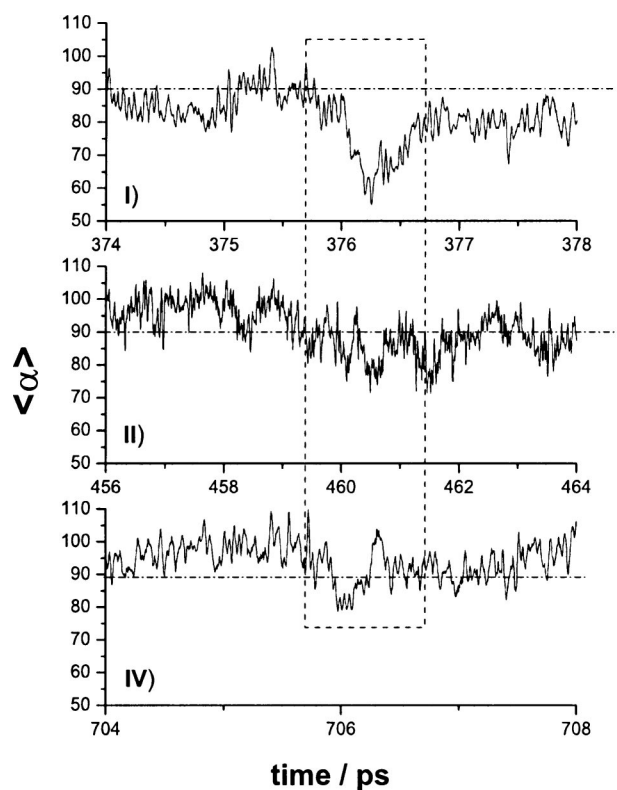The next step is to consider the water organization of

FIG. 9. Orientation angles $\langle\alpha\rangle$ for the second shell water molecules surrounding GLY residues for three different simulations (I, II, IV—see Fig. 2). The dashed rectangle illustrates the moment of β-turn formation.

residues adjacent to 2GLY. We have already encountered the water organization around 3GLY (Fig. 8, graph c1). TYR contains a polar side chain that might influence the orientation of 2GLY waters. The solvent organization around this polar group is shown in Fig. 10.

TYR can be considered as being mostly hydrophobic, except for the hydroxyl group that readily interacts with water. These characteristics are reflected in the total orientation of water molecules surrounding the TYR-OH group, since $\langle\alpha\rangle$ is randomly distributed in the first shell [Fig. 10(a)]. The standard deviation also supports this randomness.
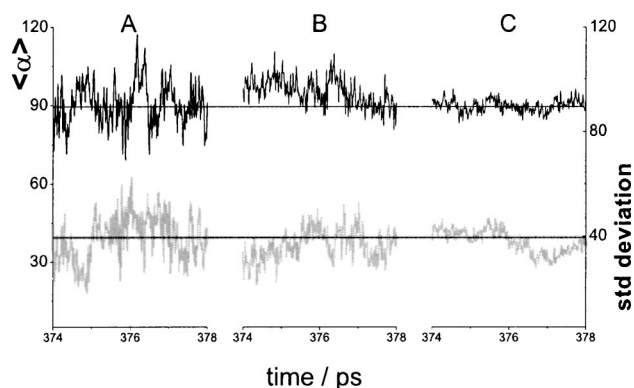

FIG. 10. $\langle\alpha\rangle$ and standard deviation of the water molecules orientation surrounding TYR-OH side-chain at (a) 3.5 Å, (b) 3–4.5 Å, and (c) 3–4.5 Å. Reference point is the hydrogen of the OH group of the side chain.
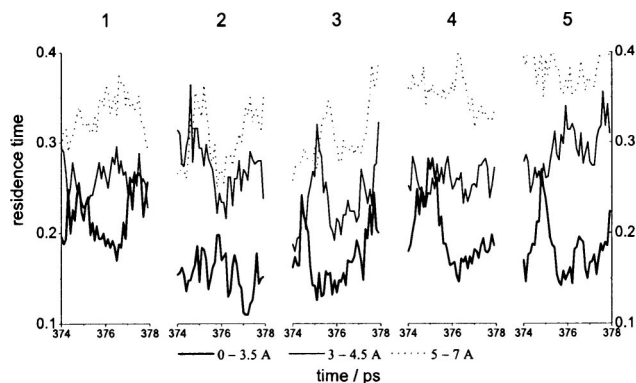
FIG. 11. Residence times of water molecules surrounding the residues at three different distances. (1) 1TYR, (2) 2GLY, (3) 3GLY, (4) 4PHE, (5) 5LEU.

E. Water mobility

In order to attain more insight into the dynamics of water close to the peptide, the water residence times were calculated. There are a number of different approaches to address this issue.[30]

The average *mobility* (or residence) of the water molecules surrounding a peptide within a given distance, over a period of 4 ps, was monitored (see Appendix C for more details). For these calculations, three different solvation shells were evaluated. One from 1.5 to 3.5 Å, one from 3 to 4.5 Å, and finally one from 5 to 7 Å.

Figure 11 illustrates the residence times of simulation I (fast "open" β-turn) for each residue in turn. At the first solvation shell most of the residues share a similar pattern, especially around the turn formation time (~375 ps). The residence times start from a low value, reach a maximum and then suddenly drop to a minimum point, indicating that the water molecules surrounding the residues "thaw" for a short period of time.

This is also the case for the residence times around the whole peptide and for the majority of the simulations (Fig. 12). Thus, this effect should be considered as general and important for the whole peptide molecule and the surrounding water network.

IV. DISCUSSION

Many soluble proteins follow a complex folding process that results in the same overall conformation, often in a reproducible manner.[31] The analysis of water dynamics appears to be fundamental to the folding event (studied here) for the following reason; in the majority of the simulations there are no strong intramolecular hydrogen bonding interactions (between the i and $i+3$ residues) that drive the dynamics leading to the β-turn, yet the turn occurs and a stable hydrogen bonding network is established. What drives this—is it the "engine," the peptide, or the water (or both)? What is the contribution of the neighboring water molecules and the water bridges towards the formation of the β-turn? We believe that the interaction of water molecules is the catalyst in the turn formation especially during the critical
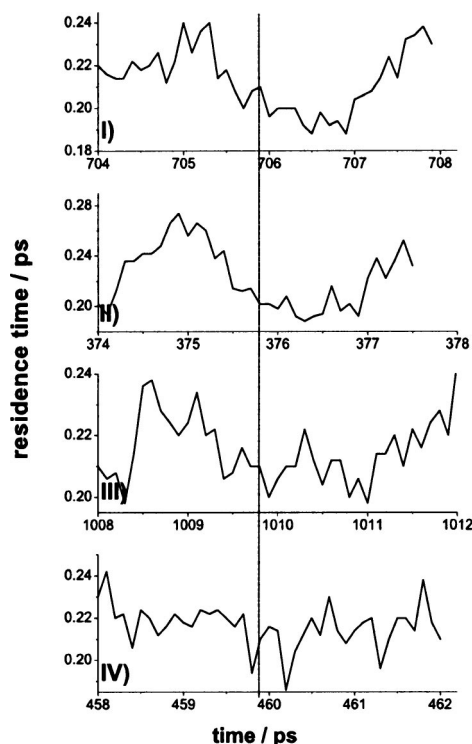

FIG. 12. Residence times of the waters surrounding the first solvation cell of the peptide during simulations I, II, III, and IV. The dotted line denotes the moment of the β-turn formation, when the water molecules become more agile (especially at the first three simulations).

moment of an open β-turn formation. We would like to emphasize that the above calculations as well as the following discussion focus solely at this critical moment. Therefore, we will concentrate on these 4 ps during which fundamental structural changes take place.

From the experimental point of view, Sakarellos *et al.*[32] determined (using NMR techniques) that neither the 2GLY-CO nor the 3GLY-CO appear to be intramolecularly hydrogen bonded in aqueous solution. Other experimental groups reported the same findings,[12] in agreement with most of our simulations. In summary, we have found that for the majority of the simulations, the peptide adopts a folded conformation (β-turn) that stays for more than 400 ps (out of 3 ns). The following discussion investigates further the solvent dynamics involved during these transitions, in terms of water orientation, time residence, water-peptide hydrogen bonding, and water bridging. At the end of the discussion we link the results together.

As already mentioned, for the majority of the β-turns there are no strong intramolecular bonds between the donors and acceptors of the i and $i+3$ residues at the moment of formation. However, we have found cases of i and $i+2$ hydrogen bonds [Figs. 3(a)–3(c)]. Apparently, these inner hydrogen bonds initially build a strong framework to bring the residues together (indicating a kind of zip-up mechanism[33]). We can assume that the flexibility of the pentapeptide constitutes the main reason for the lack of further hydrogen

bonds. Additionally, we notice (Fig. 4) that when $2 \rightarrow 5$ hydrogen bonds do take part, it is due to the contribution of a strong salt bridge. At this point we need to include solvation factors to understand further how the β-turn is formed and stabilized.

First of all, we calculated the water density, in terms of the number of water molecules, included in the inner cavity defined by the peptide's backbone for the defined critical moments of turn formation. The only clear pattern identified from these calculations was that during the formation of the fast β-turn, the water molecules reach their minimum number (sometimes zero). However, this was not the case for the slower transitions, as there was no clear correlation between the actual moment of the β-turn and a change of the number of associated water molecules.

Furthermore, Fig. 5 illustrates the general pattern for the water-peptide hydrogen bonds. As expected, most water molecules interact with the terminal residues and the number of these hydrogen bonds decreases after the formation of the turn. This is also expected as the peptide is less exposed to the solvent. Other than that, it is difficult to draw a general conclusion that relates the water-peptide hydrogen bonds with the moment of the turn formation.

The intramolecular hydrogen bonding has been based on the hydrogen bonding energies calculated by the DSSP algorithm. But when calculating the distances between donors and acceptors of energies >-1 kcal/mol (weak interaction), it came as a surprise to realize that the distances between them were ~ 4.7 Å (which is much greater than the distances usually assumed for a hydrogen bond). We understood that the reason for this weak hydrogen bonding energy is the presence of water molecules between the donor and acceptor. Consequently, Fig. 6 illustrates the significant 1TYR-4PHE and 2GLY-5LEU water bridges that stabilize the $1-4$ and $2-5$ β turns. The former water bridge stays in place for more than 2 ps and we believe that it constitutes the main reason for the *fast* formation of the β-turn. Strong water bridges were also identified in the case where intramolecular hydrogen bonding did take place. This is due to the charged terminal residues that attract a larger number of water molecules. But the timing of the later water bridges shows no correlation with the moment of the β-turn formation. Nonetheless, it is clear that for the "open" β-turns, the existence of the water bridges is important.

The α angles and their standard deviations give insight into the average orientation of the oxygen atoms of the water molecules next to each residue. We have already seen (Fig. 8, graphs a1, a2, a3) how the positively charged 1TYR induces the oxygen lone pairs of the water to point towards the residue, whereas the negatively charged 5LEU (Fig. 8, graphs e1, e2, e3) directs water oxygen lone pairs to orient away from it. Additionally, due to Coulombic effects, the standard deviation values illustrate that the waters are aligned along one direction. Of note is that none of the terminal residues show any particular change (in terms of water molecule orientation) around the moment of the turn formation.

On the other hand, the water molecules surrounding the glycines demonstrate a particular trend. Generally, the impact of their greater conformational flexibility on protein structure and enzymatic activity has been reported.[34,35] In our simulations, both glycines carry a similar number of surrounding water molecules and therefore, one would expect that the water network around 2GLY demonstrates similar features to 3GLY. On the contrary, the surrounding water molecules of one glycine (of each simulation) exhibits a rapid reorientation at the time of the β-turn formation. More specifically, around the β-turn formation, we see that $\langle \alpha \rangle$ reaches a minimum value (Fig. 8, graph b1, and Fig. 9). At the same time, the standard deviation changes suddenly from $>38.9°$ to $\ll 38.9°$. Thus, for the majority of the simulations, all water oxygens in the first solvation shell, at that particular moment, orient their lone pairs towards one of the glycines. This could be partially attributed to the small number of water molecules surrounding the particular residue, but we notice that the same pattern is seen at the second solvation shell (where the number of water molecules is significantly higher) (Fig. 9). Therefore, we believe that this is a general preference of water orientation around one of the glycines and, to our view, the most important finding of the $\langle \alpha \rangle$ calculations. We believe that this sudden reorientation of the water molecules is implicit to the whole water network rearrangement in order for the water molecules to find optimal positions for either water bridging or intramolecular hydrogen bonding.

The objective of the analysis of the water molecules residence times is to capture the local effect of the mobility of the water molecules at the time of the β-turn formation. Due to the number of different algorithms and the different molecular systems used to evaluate the protein-solvent interface residence times, there is a high variability in the results and thus it is difficult to draw general conclusions. Additionally, the small size of Leu-Enkephalin and the short period of the calculation (4 ps) makes it difficult to compare our results with the observations on water mobility analyzed in protein systems.[36,37] NMR data reveal that most of the molecules in the first water layer (including those that appear to be fixed in the crystal) are in rapid motion in solution. These results imply that water molecules near the protein surface remain very mobile with a diffusion rate similar to that of bulk water.[38] However, there are also several reports of longer residence times of the protein surface waters compared with the bulk.[39] It appears though that this can be explained by the fact that without exception, all sites with very long residence times are trapped either in cavities inside the protein or in the protein grooves. Additionally, the H-bond lifetimes between the protein and the solvent, which are a reflection of the water's residence times, can vary from 0.5 ps up to 50 ps or even more.[40] For Leu-Enkephalin, the lack of cavities (or grooves) and the existence of hydrophobic residues reduce significantly the average residence time (Fig. 11).

An additional reason for the short residence times in our simulation is the fact that most of the water molecules are close to the hydration shell boundaries. Since water molecules oscillate around the boundary region, they change solvation shells frequently and that leads to a series of many short "residence" intervals. Indeed, a close inspection of the times the water molecules spend inside a shell demonstrates two types of residence intervals: long ones, when a water

molecule resides for a considerable fraction of the 1 ps averaging period and consecutive short ones, sometimes of only a few femtoseconds long. Therefore, water mobility increases and the "survival time" becomes very small. This is more significant for the glycines, since they are associated with the least number of surrounding water molecules. Interestingly, in the second water shell, only the glycines continue to exhibit this pattern. The rest of the residues have a different water residence pattern.

Nevertheless, as far as the first solvation shell is concerned, there is an obvious pattern formed, indicating the change in the water molecules mobility when close to the moment of β-turn formation. The general pattern demonstrates a maximum value of the residence time (Figs. 11 and 12) before the β-turn, then a drop, a small fluctuation around this lower value and then, an increase after the turn is established. This is mainly for the peptide surface water molecules. When we move further from the surface, at the distance of 3–4.5 Å from each peptide atom, this pattern is lost. In order to explain the above pattern, we hypothesize that before the turn formation, the water molecules are settled in an established network. This network allows little mobility for the water. The kinetic and potential energy of the water molecules is reapportioned, followed by molecular motion which disrupts the hydrogen bonding network and allows the water molecules to establish new positions in the network. Given this hypothesis, we need to identify the causes of this disruption.

It is possible that when the two charged terminal residues come together, or when the PHE side chain moves away from the solvent, water volume is excluded from the interior of the peptide surface. Additionally, the flexibility of the glycines may be another contributor to breaking the rigidity of the water network (Fig. 8, graph b1). Around this region, the water molecules are less constrained and during a folding event they can be easily excluded towards the bulk. The water can be easily "squashed" out allowing closer peptide-peptide contacts.

We believe that the resultant water network rearrangement will lead the peptide to an optimum conformation for water bridging (when intramolecular hydrogen bonding is not present). Di Nola et al.[41] have reported how water prevents the $4 \rightarrow 1$ hydrogen bond between Met-CO and Phe-NH groups, forming a H-bonded bridge between these groups and causing a modification of the secondary structure. For the majority of our simulations, we have evidence that the water bridges are the stabilizing factors of the peptide's structure.

Summarizing our findings for the moment of the β-turn formation, we suggest the following scenario. The case of the "open" β-turn formation can be described by three stages. The first stage is characterized by a relatively high flexibility of the peptide represented by a small number of weak intramolecular H bonds and many short-lived water bridges (Fig. 6). The water network is on average oriented with the preference to be uniformly aligned next to the two charged residues. At the end of this stage, a specific network reconfiguration featuring a collective alignment of water molecules in the vicinity of the glycines (different from the rest of the peptide) takes place. This is also accompanied by a stiffening (lower mobility) of the network's surface layer around the peptide.

The second stage (376–376.2 ps) is a quick rearrangement of the water network that demonstrates a higher mobility of water molecules not only at the surface but also further from the peptide. The peptide usually forms a strong intramolecular hydrogen bond between the inner residues of the backbone and very few water bridges and displacement of water from the enclosed volume of the turn (the ends are forming a loop, restricting water access to the inner surface).

Finally, at the third stage the turn is formed, a stable 1TYR-4PHE or 2GLY-5LEU link reinforced, normally by a new water bridge. The water network reforms to its initial, predominantly uniform state.

In the case of a β-turn with intramolecular hydrogen bonding between the i and $i+3$ residues, we have seen how it is influenced by the closed structure of the terminal residues enforcing further strong intramolecular hydrogen bonds.

V. CONCLUSIONS

Through five all-atom MD simulations of Leu-Enkephalin, we have investigated in detail the moment of a β-turn formation (for a period of 4 ps). Particularly, we analyzed the influence of the water network on the folding in terms of the intramolecular hydrogen bonding pattern, the water-peptide hydrogen bonding, the orientation of the water molecules, and finally the average residence time of water molecules around the peptide. Importantly, we gave a detailed account of the role of the water hydrogen bonding network and intermolecular water bridging and how this contributes to the formation of a β-turn.

We have demonstrated how the specific water network rearrangements have led to the formation of critical water bridges that define the peptide's structure. The calculations indicate that the peptide conformation is initially stabilized by the water network which subsequently reorganizes due to increased water mobility (thaws) allowing greater peptide flexibility and establishment of a stabilizing intramolecular hydrogen bonding network consistent with an open β-turn which is subsequently stabilized by a new hydrogen bonding network of lower water mobility. Finally, we stressed the contribution of the flexible glycines to the system's rearrangement.

The phenomena described, when combined, lead to a fast transition in the peptide conformation. It should be emphasized that only the joint effect of these processes appears to drive (or allow) the motion of the peptide towards the folded conformation.

Thus, after having identified the significant water molecules involved in these critical moments, we will proceed with the complexity analysis of their dynamics that we expect will provide a fundamentally new viewpoint on the emergence of structure in the time periods of conformational transition.

ACKNOWLEDGMENTS

APPENDIX A: WATER-PEPTIDE HYDROGEN BONDING CALCULATION

To define hydrogen bonding between the water molecules and the peptide residues, we used the following geometrical criteria: strong hydrogen bonds are present when the hydrogen and the acceptor are no more than the hydrogen bonding cutoff distance apart (2.5 Å), when the D-H---A angle is at least 120° and when all H---A-R angles are at least 90°. 'H' stands for hydrogen, 'D' for donors, 'A' for acceptors and 'R' for the carbon atom bound to the acceptor.

APPENDIX B: ORIENTATION OF WATER MOLECULES

The following algorithm was applied to evaluate the changes in the water molecule orientations during the critical transitions. We selected each residue of Leu-Enkephalin and calculated the water molecules found within a distance of 1.5–3.5 Å, 3–4.5 Å, and from 5 to 7 Å, respectively. The distances were measured between the residue atom and any of the water molecule atoms within each range. Then, we defined a reference point on the peptide (typically, the hydrogen of the backbone's N-H) and calculated the angle α between two vectors: one starting at the reference point and ending at the oxygen of the water and the other, the sum of the two OH bond vectors of the water molecule. This angle was then averaged over all selected water molecules. The obtained $\langle \alpha \rangle$ represents the water orientation averaged over all water molecules within a particular shell. When $\langle \alpha \rangle < 90°$, a water oxygen's lone pairs are directed towards the reference point and when $\langle \alpha \rangle > 90°$ the lone pair points away from it.

To distinguish between the dynamics of "random" and "structured" water, the standard deviation of α in each shell was calculated. By "structured," we mean water molecules that are aligned in a similar fashion for a significant period of time. A randomly oriented water, with all angle values equally probable, will have $\langle \alpha \rangle = 90°$. Conversely, it is possible to have the same value of $\langle \alpha \rangle$ if water is structured, only this time all angles will not be equally probable but symmetrically distributed around 90°. We calculate the standard deviation in order to distinguish between these two water organizations. Randomly oriented water molecules have a standard deviation value of 39.8°. Thus, if the standard deviation is $<39.8°$, we will assign water as "structured" since it exhibits a monomodal distribution, if it is $>39.8°$ water has a multimodal distribution.[29]

APPENDIX C: WATER RESIDENCE TIME

The average *mobility* (or residence) of the water molecules surrounding a peptide within a given distance, over a period of 4 ps, was monitored. Our algorithm calculates the time periods during which a single water molecule is present within a given distance range from each residue atom. Then we average these times over the total number of water molecules found within this range. This was updated every 0.1 ps. The algorithm was applied for the total period of 4 ps. Since this is averaged over a time period, we have chosen to use a time window of 1 ps, which is long enough to contain several events of the water molecules entering, leaving, or residing within a shell.

[1] I. D. Kuntz and W. Kauzmann, Adv. Protein Chem. **28**, 239 (1974). J. L. Rupley, E. Gratton, and G. Careri, Trends Biochem. Sci. **8**, 18 (1983).

[2] S. K. Pal, J. Peon, and A. H. Zewail, Proc. Natl. Acad. Sci. U.S.A. **99**, 1763 (2002).

[3] D. Beck, D. Alonso, and V. Daggett, Biophys. Chem. **100**, 221 (2003).

[4] J. M. Sorenson, G. Hura, A. K. Soper, A. Petsemlidis, and T. Head-Gordon, J. Phys. Chem. B **103**, 5413 (1999).

[5] A. E. Garcia and G. Hummer, Proteins: Struct., Funct., Genet. **38**, 261 (2000).

[6] S. Dennis, C. J. Camacho, and S. Vajda, Proteins: Struct., Funct., Genet. **38**, 176 (2000).

[7] R. L. Baldwin, Biophys. Chem. **101−102**, 203 (2002).

[8] S. M. Bhattacharyya, Z. Wang, and A. H. Zewail, J. Phys. Chem. B **107**, 132118 (2003).

[9] P. E. Smith and B. M. Pettitt, J. Phys. Chem. **98**, 9700 (1994); M. A. Khaled, M. M. Long, W. D. Thompson, R. J. Bradley, G. B. Brown, and D. W. Urry, Biochem. Biophys. Res. Commun. **76**, 224 (1977); E. R. Stimson, Y. C. Meinwald, and H. A. Scheraga, Biochemistry **18**, 1661 (1979); G. Gupta, M. H. Sarma, and M. M. Dhingra, FEBS Lett. **198**, 245 (1986); A. Motta, T. Tancredi, and P. A. Temussi, *ibid.* **215**, 215 (1987).

[10] M. H. Zaman, M. Shen, R. S. Berry, and K. F. Freed, J. Phys. Chem. B **107**, 1685 (2003); K. J. Jalkanen, J. Phys.: Condens. Matter **15**, S1823 (2003); S. Abdali, M. Ø. Jensen, and H. Bohr, *ibid.* **15**, S1853 (2003).

[11] J. Hughes, T. W. Smith, H. W. Kosteriltz, L. A. Fothergill, B. A. Morgan, and H. R. Morris, Nature (London) **258**, 577 (1975).

[12] D. van der Spoel and H. J. C. Berendsen, Biophys. J. **72**, 2032 (1997).

[13] M. Aburi and P. E. Smith, Biopolymers **64**, 177 (2002).

[14] S. Abdali, M. Jensen, and H. Bohr, J. Phys.: Condens. Matter **15**, S1853 (2003).

[15] D. Nerukh, G. Karvounis, and R. C. Glen, J. Chem. Phys. **117**, 9611 (2002).

[16] P. E. Smith and B. M. Pettitt, J. Am. Chem. Soc. **113**, 6029 (1991).

[17] SYBYL [molecular modeling package], version 6.8, Tripos Associates, St Louis, MO, 2000.

[18] H. J. C. Berendsen, J. P. M. Postma, W. F. van Gunsteren, and J. Hermans, in Intermolecular Forces, edited by B. Pullman (Reidel Dordrecht, 1981), pp. 331–342.

[19] W. R. P. Scott, P. H. Hunenberger, I. G. Tironi *et al.*, J. Phys. Chem. A **103**, 3596 (1999).

[20] W. F. van Gunsteren and H. J. C. Berendsen, Angew. Chem., Int. Ed. Engl. **29**, 992 (1990).

[21] J. P. Ryckaert, G. Ciccotti, and H. J. C. Berendsen, J. Comput. Phys. **23**, 327 (1977).

[22] S. Miyamoto and P. A. Kollman, J. Comput. Chem. **13**, 952 (1992).

[23] E. G. Hutchinson and J. M. Thornton, Protein Sci. **5**, 212 (1996).

[24] E. N. Baker and R. E. Hubbard, Prog. Biophys. Mol. Biol. **44**, 97 (1984).

[25] K. D. Berndt, P. Güntert, and K. Wüthrich, J. Mol. Biol. **234**, 735 (1993).

[26] W. Kabsch and C. Sander, Biopolymers **22**, 2577 (1983).

[27] S.-Y. Sheu, D.-Y. Yang, H. L. Selzle, and E. W. Schlag, Biophysics (Engl. Transl.) **100**, 12683 (2003).

[28] K. C. Chou, Anal. Biochem. **286**, 1 (2000); C. M. Wilmot and J. M. Thornton, J. Mol. Biol. **203**, 221 (1988); C. M. Wilmot and J. M. Thornton, Protein Eng. **3**, 479 (1990).

[29] A. M. Bujnowski and W. G. Pitt, J. Colloid Interface Sci. **203**, 47 (1998).

[30] A. R. Bizzarri and S. Cannistraro, J. Phys. Chem. B **106**, 6617 (2002).

[31] C. M. Dobson, Semin Cell Dev. Biol. **15**, 3 (2004); V. Daggett and A. Fersht, Nat. Rev. Mol. Cell Bio **4**, 497 (2003).

[32] A. Aubry, N. Birlirakis, M. Sakarellos-Daitsiotis, C. Sakarellos, and M. Marraud, Biopolymers **28**, 27 (1989).

[33] P. Ferrara and A. Caflisch, J. Mol. Biol. **306**, 837 (2001).

[34] M. Okoniewska, T. Tanaka, and R. Y. Yada, Biochem. J. **349**, 169 (2000).

[35] B. X. Yan and Y. Q. Sun, J. Biol. Chem. **272**, 3190 (1997).

[36] A. E. Garcia and L. Stiller, J. Comput. Chem. **14**, 1396 (1993).

[37] C. Rocchi, A. R. Bizzarri, and S. Cannistraro, Chem. Phys. **214**, 261 (1997).

[38] V. A. Vladimir, B. K. Andrews, P. E. Smith, and B. M. Pettitt, Biophys. J. **79**, 2966 (2000).

[39] K. Modig, E. Liepinsh, G. Otting, and B. Halle, J. Am. Chem. Soc. **126**, 102 (2004); D. Russo, P. Baglioni, E. Peroni, J. Teixeira, Chem. Phys. **292**, 235 (2003).

[40] A. R. Bizzarri, C. X. Wang, W. Z. Chen, and S. Cannistrato, Chem. Phys. **201**, 463 (1995).

[41] A. Di Nola, E. Gavuzzo, F. Mazza, G. Pochetti, and D. Roccatano, J. Phys. Chem. **99**, 9625 (1995).